# Protection of the structural materials of MSR through Ni-coating

Younghwan Jeon [a, b], Kyeongtae Park [b], Jaeyeong Park [b*]

[a]*Advanced Fuel Cycle Technology Division, Korea Atomic Energy Research Institute, 111, Daedeok-daero 989beon-gil, Yuseong-gu, Daejeon, 34057, Republic of Korea*
[b]*Department of Nuclear Engineering, Ulsan National Institute of Science and Technology, 50 UNIST-gil, Ulju-gun, Ulsan 44919, Republic of Korea*
[*]*Corresponding author: jypark@unist.ac.kr*

***Keywords :*** Molten salt reactor, Ni-coating, molten salt corrosion, electrochemistry

## 1. Introduction

A molten salt reactor (MSR) is one of the promising GEN-IV reactors that utilize molten salt as its coolant and fuel. MSRs particularly offer inherent safety features, high efficiency, and the potential for compact design. Due to these advantages, various countries and companies are developing MSRs, and Korea also developing the chloride-based MSRs. Many new studies are required to develop the MSRs such as core analysis, reactor design, thermal-fluid analysis, and salt properties analysis.

The biggest problem in the development of MSRs is the molten salt corrosion of the structural materials due to the highly corrosive salts. Molten salt corrosion in MSR environments is evoked by various mechanisms; electrochemical redox reaction ($2U^{4+}+Cr \rightarrow 2U^{3+}+Cr^{2+}$), humidity and oxygen impurities in salt, and fission products induced chemical reactions [1-5]. To mitigate the molten salt corrosion, much research to remove $H_2O$ and $O_2$ from the salt [3] and control the fission products were conducted [4, 5] and redox potential control techniques such as sacrificial metal injection and $U^{4+}/U^{3+}$ ratio control were studied [1, 2]. However, it was verified that the electrochemical redox potential control techniques can mitigate the molten salt corrosion, but not completely suppress it.

In many researches, pure Ni showed better corrosion resistance to the molten salt than the Ni-based alloys but, pure Ni has poor mechanical properties and corrosion behaviors in air conditions than many conventional alloys. It was expected that the structural materials that coated with Ni on the salt-contact side can endure the molten salt corrosion with sufficient mechanical properties and corrosion due to the air. Herein, molten salt corrosion behaviors of the Ni-coated Ni-based alloy in various scenarios were investigated.

## 2. Experimental Setup

### *2.1 Sample preparation*

Five corrosion specimens were prepared, encompassing Ni-based alloy (80Ni–20Cr), pure Ni, Ni-coated Ni-based alloy, damaged Ni-coated Ni-based alloy, and half Ni-coated Ni-based alloy. The Ni-based alloy and pure Ni sheets were machined by using electrical discharge machining (EDM) and polished with SiC paper to a grit of 2000 before the corrosion experiments and the Ni-coating process. The shape of the corrosion specimens is described in Fig. 1 (a).

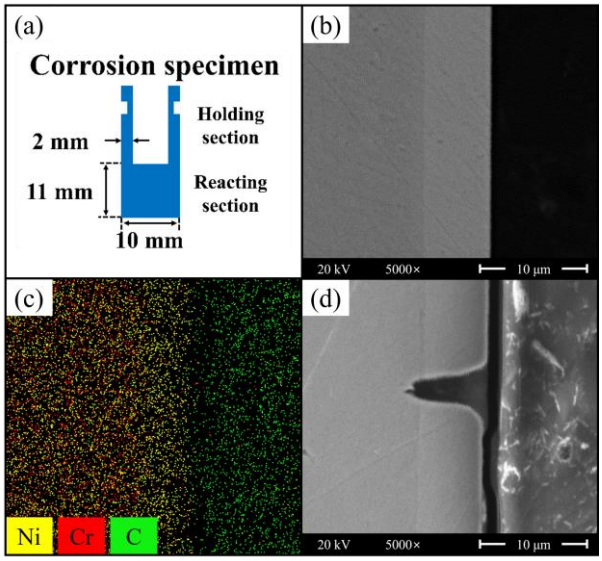


Fig. 1. Schematics of the corrosion specimen (a), cross-sectional SEM–EDS images of the Ni-coated Ni-based alloy (b, c), and cross-sectional SEM image of the damaged Ni-coated Ni-based alloy (d)

The Ni-coating process was conducted through electrochemical methods in a water-based solution composed of 250 g $L^{-1}$ $NiSO_4 \cdot 6H_2O$, 35 g $L^{-1}$ $H_3BO_3$, and 40 g $L^{-1}$ $NiCl_2 \cdot 6H_2O$ and the pH value of the solution was adjusted to 3.5 using an ammonia solution [6, 7]. All coating processes were performed under 6 mA $cm^{-2}$ conditions for a duration of 2580 seconds at 55 ℃ to form the 5 μm-thickness of Ni-layer (Fig. 1 (b, c)). In a separate procedure, Ni-coating was conducted under the same conditions after attaching a conductive Cu tape to Ni-based alloy specimens, and the tape was removed to make the half Ni-coated Ni-based alloy specimens. To manufacture the damaged Ni-coated Ni-based alloy specimens, the Ni-coated Ni-based alloy

underwent ion milling processes by using a focused ion beam (FIB) and 3 micro-cracks of 500 μm×3 μm×7 μm were generated on each specimen (Fig. 1 (d)).

### *2.2 Corrosion cell configuration*

All salt reagent preparation and corrosion experiments were conducted in a glove box filled with Ar gas and its moisture and oxygen contents were rigorously maintained below 0.1 ppm during the experiments. The NaCl (Alfa Aesar, 99.99%) and $MgCl_2$ (Alfa Aesar, 99.99%) salts were pre-heated at 200 ℃, 400 ℃, and 600 ℃ for 24 hours to remove residual moisture and oxygen in the salt and were mixed with eutectic composition of 58.0 at% NaCl–42.0 at% $MgCl_2$. A flat-bottomed cylindrical boron nitride (BN) tube its inner diameter and height were 30 mm was used as the crucible and 15.000 g of NaCl–$MgCl_2$ salt was utilized in each experiment. It was verified that the reacting section of the corrosion specimens was fully submerged and less than 1 mm depth of the connecting section of the specimen was immersed.

The 700 ℃ condition was selected as the corrosion experiments temperature and the temperature was controlled by the PID controller attached to the electrical furnace. A dummy cell filled with NaCl–$MgCl_2$ was positioned at the center of the furnace, enabling temperature measurement and verification of temperature maintenance throughout the experiments. At the end of the corrosion experiments, the corrosion cell was withdrawn from the furnace before the salt solidified. Subsequently, specimen extraction and salt separation from the BN crucible were carried out.

### *2.3 Experimental procedures*

The corrosion experiments were conducted on the five specimens prepared in Section 2.1 and the corrosion periods were set as the 3, 7, 14, and 21 days (Table I). Prior to being introduced into the corrosion experiment, each specimen was cleaned with ethyl alcohol, then vacuum-dried, and the weight of each specimen was measured using an electronic balance. After the experiments, the specimens were extracted from the corrosion cell, then subjected to ultrasonic cleaning in DI water for 200 minutes, vacuum-dried, and the weight of the specimens was measured to assess their weight changes. The solidified salt was crushed using a mortar and approximately 0.2 g of salt was used to measure its alloying element contents by using ICP-OES.

Table I: Experimental procedures for the corrosion experiments

| Test ID | Corrosion duration | Note |
|---|---|---|
| S-3 | 3 days | Un-coated |
| S-7 | 7 days | 80Ni–20Cr |
| S-14 | 14 days | |
| S-21 | 21 days | |
| N-3 | 3 days | Pure Ni |
| N-7 | 7 days | |
| N-14 | 14 days | |
| N-21 | 21 days | |
| C-3 | 3 days | 5 μm-Ni-coated 80Ni–20Cr |
| C-7 | 7 days | |
| C-14 | 14 days | |
| C-21 | 21 days | |
| D-3 | 3 days | Ni-coated 80Ni–20Cr with 3 micro-cracks |
| D-7 | 7 days | |
| D-14 | 14 days | |
| D-21 | 21 days | |
| H-3 | 3 days | Half Ni-coated 80Ni–20Cr |
| H-7 | 7 days | |
| H-14 | 14 days | |
| H-21 | 21 days | |

The microstructural changes of the specimens were analyzed by observing their surface and cross-section using SEM–EDS. After the analysis of the surface, the specimen was cut, vertically fixed with embedding clips, and placed on a graphite mount. Mounted specimens were polished and the final step was done with 1 μm $Al_2O_3$ suspension. For the damaged Ni-coated Ni-based alloy specimens (Test ID: D), an appropriate milling thickness was achieved using micrometers during the polishing process, specifically to observe cracks generated by FIB.

## 3. Results

### *3.1 Mass and salt contents change after the corrosion experiments*

The weight changes of specimens and the contents of Ni and Cr in the salt after the corrosion experiments are presented in Fig. 2 (a) and the corrosion rates normalized to the corrosion rate of the Un-coated Ni-based alloy (Test ID: S) are presented in Fig. 2 (b). The corrosion rates were severe in the order of Test ID N, C, D, H, and S. In the corrosion test of the Un-coated Ni-based alloy, analyzed Ni contents were lower than the detection limit of ICP-OES whereas the trace amounts of Ni were detected after the C, D, and H experiments. Particularly in specimens C and D, it was noted that the Ni concentration on days 14 and 21 was lower than that on days 3 and 7. For specimens C and D, the corrosion rates remained below 20% and 25%, respectively, during the initial 7 days but sharply increased to approximately 35% and 40%, respectively, after 14 days of specimens.

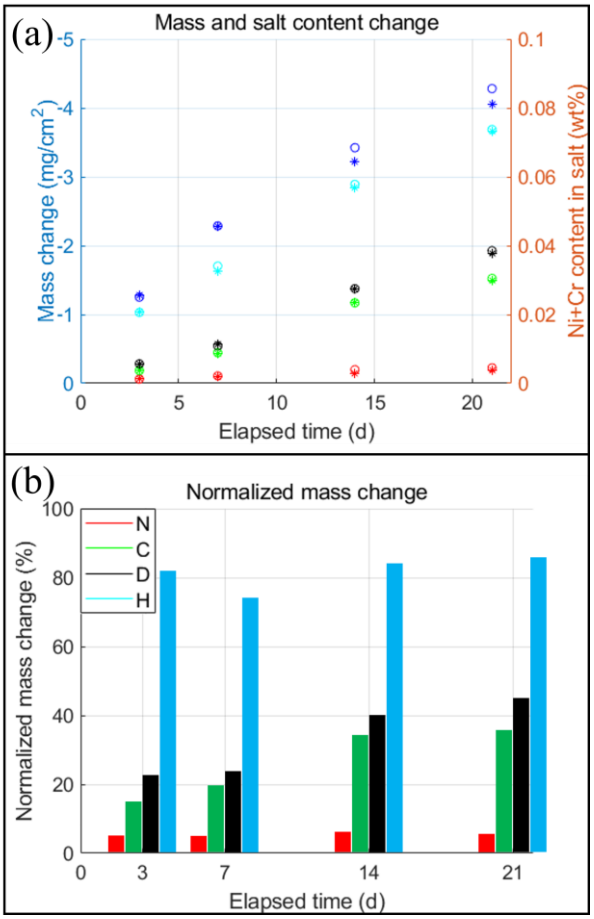


Fig. 2. Mass and salt content changes after the corrosion experiments (a) and normalized mass change by the mass change of un-coated Ni-based alloy after the corrosion experiments (b)

### *3.2 Microstructural changes after the corrosion experiments*

After the corrosion experiments, the surface and cross-section of each specimen were observed using SEM–EDS. The cross-sectional SEM images of S-21 and N-21 specimens are shown in Fig. 3. Corrosion rate of the pure Ni was much lower than that of the 80Ni–20Cr alloy.

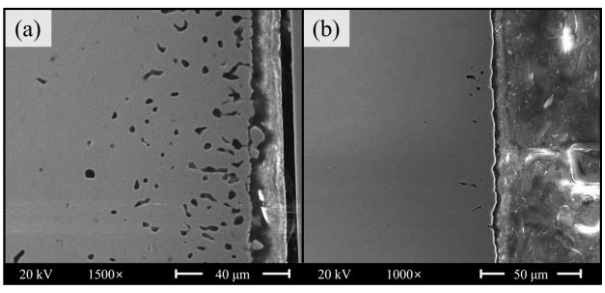


Fig. 3. Cross-sectional SEM images of S-21 (a) and N-21 specimens (b)

In the presence of the Ni-coated layer, the Ni-layer corroded preferentially and protects the base metal (Fig. 4 (a)). However, base metal suffers molten salt corrosion when the base metal is exposed to the molten salt due to the corroded Ni-coated layer (Fig. 4 (b)).

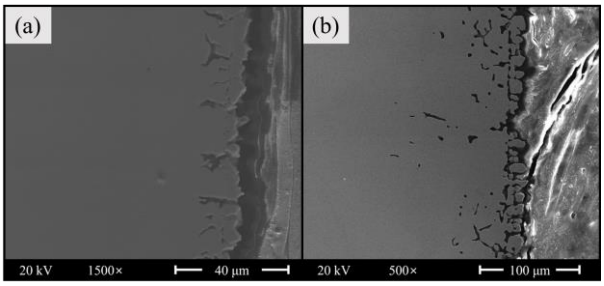


Fig. 4. Cross-sectional SEM images of C-7 (a) and C-21 specimens (b)

In the case of D-series specimens which have micro-cracks on the Ni-coated layer, pitting corrosion below the micro-cracks were observed (Fig. 5). The size of the pits was grown as corrosion duration increases.

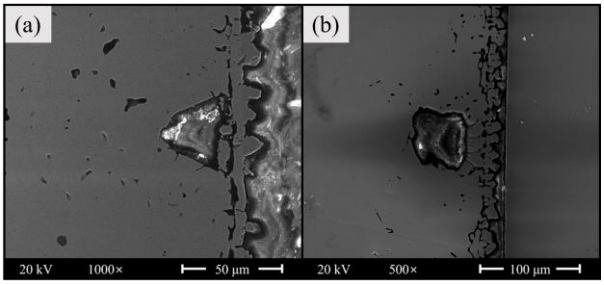


Fig. 5. Cross-sectional SEM images of D-14 (a) and D-21 specimens (b)

For the H-series specimens which simulate the extensive damage on the Ni-coated layer, crevice corrosion was observed at the edge of the Ni-coated layer (Fig. 6). Also, the maximum corrosion depth of the uncovered alloy region was much deeper than that under the Ni-layer.

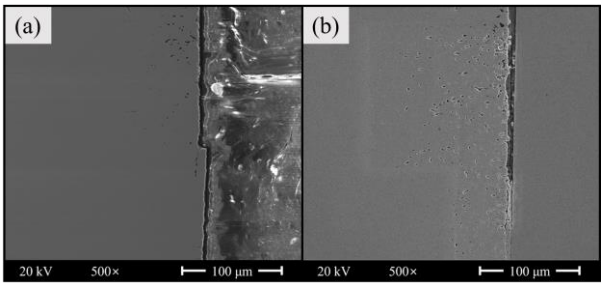


Fig. 6. Cross-sectional SEM images of H-7 (a) and H-21 specimens (b)

## 4. Discussion

### *4.1 Protection of structural materials from molten salt corrosion via Ni-coating*

It was confirmed that the corrosion rate of the Ni-coated Ni-based alloy with intact Ni-coated layer was approximately lower than 25% than uncovered Ni-based alloy which implies that the corrosion inhibition can be achievable through Ni-coating. However, the corrosion rate was increased after the Ni-coated layer was damaged. Additionally, similar to the results of the Half-Ni-coated Ni-based alloy corrosion experiments, it was confirmed that the base metal beneath the Ni-layer is sufficiently protected from molten salt corrosion. However, when the Ni-coated layer is corroded and damaged, the Ni-layer fails to protect the base metal from the molten salt corrosion which results in corrosion of the base metals.

According to the mass changes of the Ni-coated Ni-based alloy experiments, the molten salt corrosion rate of the Ni-coated layer can be derived and is approximately 25–26 μm $y^{-1}$. Based on these results, about 800 μm-thick Ni-layer would be required to protect the structural materials from molten salt corrosion.

### *4.2 Changes in molten salt corrosion behaviors due to damaged Ni-coated layer*

After the corrosion experiments, high-purity Ni particles were observed on the surface of the Ni-coated specimens; C, D, and H series. Additionally, Ni contents in the salt after the C-3 and C-7 experiments were higher than those after the C-14 and C-21 experiments. These phenomena are evoked due to the reaction of Cr in 80Ni–20Cr alloy and $Ni^{2+}$ ion in the salt which is the corrosion products ($Ni^{2+} + Cr \rightarrow Ni + Cr^{2+}$) during the experiments. On the other hand, in cases of D series or H series experiments, the base metal was exposed to the molten salt from the beginning of the corrosion experiment. Consequently, $Ni^{2+}$ ions from the Ni-coated layer rapidly reacted with the exposed base metal causing the pitting or crevice corrosion.

## 5. Conclusion

In this study, it was confirmed that a robust Ni-coated layer effectively protects the structural materials from molten salt corrosion. Especially when the Ni-coated layer was intact, corrosion rates were less than 20% compared to those of the 80Ni–20Cr alloy. However, when the Ni-coated layer is damaged due to molten salt corrosion or other factors, the corrosion rate increases dramatically. Additionally, pitting corrosion and crevice corrosion which were rarely reported in other studies were observed when the Ni-coated layer had intensive or extensive damage.

## Acknowledgment

This study was supported by a National Research Foundation of Korea (NRF) grant funded by the Ministry of Science and ICT, Republic of Korea (NRF-2022M2D2A1A02063129).

## REFERENCES

[1] R. Roper, M. Harkema, P. Sabharwall, C. Riddle, B. Chisholm, B. Day, P. Marotta, Molten salt for advanced energy applications: A review, Annals of Nuclear Energy, Vol. 169, p. 108924, 2022.
[2] J. Zhang, C.W. Forsberg, M.F. Simpson, S. Guo, S.T. Lam, R.O. Scarlat, F. Carotti, K.J. Chan, P.M. Singh, W. Doniger, Redox potential control in molten salt systems for corrosion mitigation, Corrosion Science, Vol. 144, pp. 44-53, 2018.
[3] V. Afonichkin, A. Bovet, V. Shishkin, Salts purification and voltammetric study of the electroreduction of U (IV) to U (III) in molten LiF–ThF4, Journal of nuclear materials, Vol. 419, pp. 347-352, 2011.
[4] O. Beneš, E. Capelli, N. Morelová, J.-Y. Colle, A. Tosolin, T. Wiss, B. Cremer, R. Konings, Cesium and iodine release from fluoride-based molten salt reactor fuel, Physical Chemistry Chemical Physics, Vol. 23, pp. 9512-9523, 2021.
[5] L. Chen, L.-Y. He, B. Zhou, G.-F. Zhu, Y.-H. Fan, H.-J. Xu, R. Yan, Y. Zou, Evaluation on 131I production based on molten salt reactor off-gas extraction, Annals of Nuclear Energy, Vol. 195, p. 110192, 2024.
[6] H. Jin, Y.-Y. Wang, Y.-T. Wang, H.-B. Yang, Synthesis and properties of electrodeposited Ni–CeO 2 nano-composite coatings, Rare Metals, Vol. 37, pp. 148-153, 2018.
[7] A. Rashidi, A. Amadeh, Effect of electroplating parameters on microstructure of nanocrystalline nickel coatings, Journal of Materials Science & Technology, Vol. 26, pp. 82-86, 2010.